Partial Differential Equations in Applied Mathematics 11 (2024) 100829

Contents lists available at ScienceDirect

Partial Differential Equations in Applied Mathematics

journal homepage: www.elsevier.com/locate/padiff

Hemodynamic characteristics of blood flow in an inclined overlapped stenosed arterial section☆

Mallinath Dhange [a,*], Gurunath Sankad [a], Umesh Bhujakkanavar [b], Kusal K Das [c], J.C. Misra [d]

[a] Department of Mathematics, BLDEA's VP Dr. PG Halakatti College of Engineering and Technology, (Affiliated to Visvesvaraya Technological University, Belagavi), Vijayapur 586103, India
[b] Department of Science and Humanities, Rajarambapu Institute of Technology, Islampur 415414, Maharashtra, India
[c] Department of Physiology, Laboratory of Vascular Physiology and Medicine, Shri B.M. Patil Medical College, Hospital and Research Centre, BLDE (Deemed to be University) Vijayapur, India
[d] Indian Institute of Engineering Science and Technology, Shibpur, West Bengal, India

ARTICLE INFO

Keywords:
Casson fluid
Overlapping stenosis
Flow resistivity
Shear stress
Proclivity angle

ABSTRACT

This work presents a theoretical analysis of the non-linear behavior of blood flow along an angled arterial section with overlapping stenosis. An elastic cylindrical tube with a moving wall is used to represent the artery, and a Casson liquid is used to simulate blood flowing through it. The nonlinear equations that govern blood flow are taken into account. The influence of the pulsatile pressure gradient caused by the regular heartbeat on the flow process in the stenosed artery is demonstrated mathematically. The current analytical method can compute the wall shear stress, flow resistivity, and velocity profiles with mild stenosis assumption by applying the boundary conditions. Numerical calculations of the desired quantities are carried out systematically. They provide an overview of how the degree of stenosis and the malleability of the artery wall influence blood flow abnormalities. Concerning the height of stenosis, the surface shear stress and the resistivity to flow increase together with an increase in the proclivity angle.

1. Introduction

One of the diseases affecting the human cardiovascular system is the constriction of blood arteries brought on by improper tissue development. As a result, blood flow may be decreased or obstructed, which might result in significant cardiovascular diseases. One of the most significant causes of death in the developed world today is cardiovascular disease. The cardiovascular system, which is made up of the heart and blood arteries, is what allows blood to flow via an artery. Vascular conditions may significantly change how blood flows. Blood vessels and heart conditions, such as heart attacks and strokes, face serious health hazards today and are responsible for a significant portion of mortality. The properties of blood flow and vascular behavior are directly related to these diseases. These deaths are mostly due to stenosis. The term "stenosis" describes the narrowing of an artery as a result of the development of arteriosclerotic plaques or another kind of abnormal tissue growth. It has been suggested that deposits of fatty material, cholesterol, and cellular waste products on the arterial wall are the causes of stenosis, even if the exact causes remain unclear. When an artery develops stenosis, blood flow is decreased. The usual working of the circulatory system may be impaired by injuries sustained by the occurrence of stenosis in an artery. In particular, heart attacks might happen as a consequence of it. Blood flow restriction can injure the inner cells of the wall and hasten the onset of stenosis. Therefore, there is a link between the development of stenosis and blood flow in the artery since one affects the other. Young[1] was the first to study stenosis and looked at how it affected the steady flow of blood through a pipe. Models of the flow patterns in stenosed blood arteries were created by Azuma and Fukushima.[2] Vascular stenosis' impact on steady flow was mentioned by MacDonald.[3] Then, several research examined the flow characteristics of blood in a pipe with mild contraction using blood under various conditions such as Newtonian or non-Newtonian fluids.[4–12]

Through the use of a mathematical model, Chakraborty and Mandal[13,14] investigated the blood flow in overlaying stenosis with body acceleration. Two-layered non-Newtonian flow and overlapping stenosis's impact on arterial flow have both been studied by Srivastava et al.[15,16] In the context of overlapping stenosis, the arterial flow was

☆ Subject classification codes: 76Z05, 92C10.
* Corresponding author.
E-mail address: math.mallinath@bldeacet.ac.in (M. Dhange).

https://doi.org/10.1016/j.padiff.2024.100829
Received 1 February 2024; Received in revised form 13 July 2024; Accepted 17 July 2024
Available online 18 July 2024

Nomenclature

L	length of the tube (m)
L_0	length of stenosis (m)
d	Beginning of the stenosis region
δ	maximum height of stenosis (m)
u	Velocity of fluid (m/s)
u_p	Velocity of fluid in plug flow region (m/s)
r	radial coordinate (m)
θ	the angle of proclivity ($radian$)
$R(z)$	radius of the artery (m)
R_0	the radius of the normal artery (m)
p	pressure across the region (kg/ms^2)
h	Length of the geometry of artery wall (m)
$\overline{\lambda}$	resistance to the flow (kg/m^4s)
$\overline{\tau}_w$	wall shear stress (N/m^2)
τ_{rz}	shear stress (N/m^2)
μ	blood viscosity (kg/ms)
τ_0	yield stress (N/m^2)
g	acceleration due to gravity (m/s^2)
H	Length of the geometry of artery wall (m)
R_p	Radial distance in plug flow region (m)
r_0	Radial distance (m)
Q	volume flow rate (kW/m^2)
ρ	the density of the fluid (kg/m^3)
z	axial coordinate (m)

examined by Riahi et al.[17] Mathematical modeling of irregular blood flow through elastic tapering arteries with overlapping stenosis was explored by Haghighi et al.[18] Following that, other studies investigated the effects of overlapping stenosis in blood flow through varied artery geometry.[19–24]

Non-Newtonian blood flow has recently attracted the attention of scientists because it can be used to study blood flow via constricted arteries. Most investigations in the literature employ the Herschel-Bulkley, micropolar, Jeffrey, and Newtonian models. Due to the presence of yield stress, this technique is unable to explain the physiological behavior of the circulation in feeding channels. The Casson model resembles the blood moving at low shear rates better than the Herschel-Bulkley fluid, despite the latter's yield stress constraint (see ScottBlair[25]). Recently, multiple researchers examined Casson fluid under various physiological conditions.[26–29]

It is well known that many pipes in physiological systems are inclined to the axis rather than horizontally. By Prasad and Radhakrishnamacharya,[30] the blood flow via an artery with many stenoses and an uneven cross-section was investigated. An inclined elastic tube with a permeable wall and a creeping Casson liquid flow were studied by Gudekote and Choudhari.[31] According to Umadevi et al.[32] copper nanoparticles and a magnetic force paired with an interwoven, restricted oblique artery were used to study the blood flow. The Casson fluid model for blood flow through an inclined tapered artery of an accelerated body in the presence of MHD is explored by Srivastava.[33] Gupt and Gupta[34] observed the unsteady blood flow in an artery through a non-symmetrical stenosis. Pralhad and Scultz[35] investigated arterial stenosis through modeling and its application to blood diseases. A mathematical model for different shapes of stenosis and slip velocity at the wall through mild stenosis artery is explored by Kumar et al.[36] Recently, several scientists examined the characteristics of blood flow within an artery in the presence of stenosis.[37–51]

This study's challenge may be used in engineering and biomedical applications. The literature evaluation indicates that numerous researchers have studied the stenosed artery. Although treating blood as Casson fluid, no study has yet demonstrated how the angle of proclivity affects blood flow in an overlapping stenosed artery. Using the inspiration from the foregoing work, an attempt was made to investigate the effects of overlapping stenosis on a Casson fluid under mild stenosis conditions. Diagrams are used to show how various significant limitations affect the flow of energy, and formulas are generated for velocity, flow resistance, and wall shear stress.

2. Mathematical formulation and solution

Take into account the movement of a Casson fluid that is incompressible through a conduit that has a uniform cross-section and an inclined axisymmetry overlap. The stenosis should be modest and progress axially symmetrically. The surface's geometry is shown in Fig. 1.

The formula involving the geometry of the stenosed surface is (Chakraborty and Mandal,[13] Srivastava et al.[15])

$$h=\frac{R(z)}{R_0}=\begin{cases}1-\dfrac{3\delta}{2R_0L_0^4}\left[\begin{array}{c}11(z-d)L_0^3-47(z-d)^2L_0^2+\\ 72(z-d)^3L_0-36(z-d)^4\end{array}\right] & : d\le z\le d+L_0\\ 1\ : otherwise & \end{cases}. \tag{2.1}$$

Here, the tube's radius at the stenotic area is $R(z)$, the radius of the artery's normal segment is R_0, the start of the stenotic area lies at position d, and the tube length is L. L_0measures how long the stenotic area and the proclivity angle is θ. As measured from the origin, $\delta$is the maximum height of the stenosis at $z=d+L_0/6$, $z=d+5L_0/6$, and $\frac{3\delta}{4}$ is the critical height of the stenosis at $z=d+\frac{L_0}{2}$, and the length of overlapping stenosis is h.

2.1. Leading equations

In this learning, lifeblood was taken to be a consistent, incompressible, non-Newtonian liquid. The viscidness of lifeblood can be described by a collection of non-Newtonian liquid prototypes, together with the micropolar, Herschel-Bulkley, power-law liquid schemes, and others. We utilized the Casson liquid prototypical to characterize the physical property of blood in our study because, when matched to other viscosity

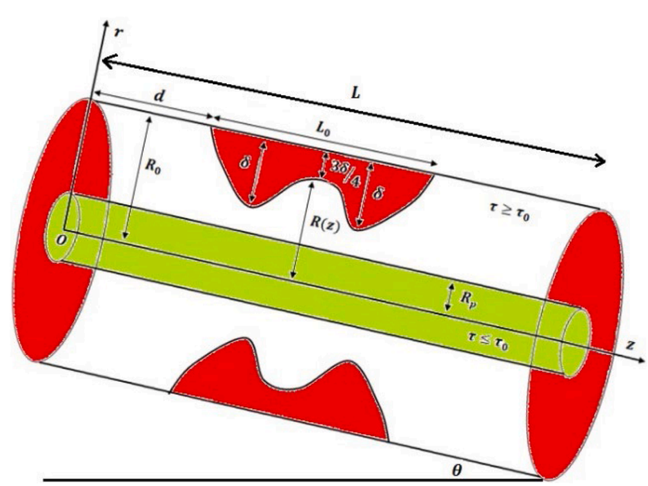

Fig. 1. Design of overlying stenosis.

prototypes, it exactly depicts the viscidness characteristic of physiological blood in day-to-day lifespan (Pratumwal et al.[41]).

According to Prasad and Radhakrishnamacharya,[30] Vajravelu et al.[42] Chaturani and Ponalugusamy[43] the important formulation of the flowing for the existing circumstances is as follows:

$$\frac{1}{r}\frac{\partial}{\partial r}(r\,\tau_{r\,z}) = \rho g sin\theta - \frac{\partial p}{\partial z}, \tag{2.1.1}$$

where,

$$\begin{cases} \sqrt{\tau_{r\,z}} = \sqrt{\mu}\sqrt{-\dfrac{\partial u}{\partial r}} + \sqrt{\tau_0} & : \tau_{r\,z} \geq \tau_0 \\ -\dfrac{\partial u}{\partial r} = 0 & : \tau_{r\,z} \leq \tau_{0.} \end{cases} \tag{2.1.2}$$

Here, θ is the proclivity angle, $\tau_0$is the yield stress, μis the blood viscosity, τ_{rz} is the shear stress, *p*is the pressure, *u*is the velocity of the fluid, *g*is the acceleration due to gravity, ρis the density of the fluid, and (z, r) are the correspondingly axial and radial coordinates.

2.2. Borderline conditions (BC) and mathematical solution

Boundary constraints play a key role in computing the solutions to simulated physical issues. Since lifeblood elements stick to the interior surface of the questioned artery piece, it may be inferred that the axial speed (u) of blood elements on the surface, matches to one-dimensional stream, and is identical to the swiftness of arterial barrier material. The quantitative description of the stenosed portion of this is as follows and it is also called the no-slip boundary condition:

$$u = 0 \; at \; r = h. \tag{2.2.1}$$

Supposing that there is no liquid shear rate along the axis of the artery section in the problem, the fluid stream speed gradient along the axis can be written as:

$$\tau_{rz} \text{ is finite at } r = 0. \tag{2.2.2}$$

The velocity of the fluid is determined by taking into account the constraint for mild stenosis and addressing (2.1.1) within the boundary constraints (2.2.1) and (2.2.2) as:

$$u = \left[\frac{4}{3}r_0^{\frac{1}{2}}\left(r^{\frac{3}{2}} - h^{\frac{3}{2}}\right) - \frac{1}{2}\left(r^2 - h^2\right) - r_0(r-h)\right]\frac{\left(-\frac{\partial p}{\partial z} + f\right)}{2\mu}. \tag{2.2.3}$$

where $F = \frac{\mu\, c^{\frac{1}{2}}}{\rho\, g\, R_0^{\frac{3}{2}}}$, $f = \frac{sin\theta}{F}$, c is the moving wave speed (see ref. Vajravelu et al.[42] of the arterial wall.

Using $\frac{\partial u}{\partial r} = 0$ of Eq. (2.1.2), we obtain the upper limit of the plug flow region i. e. the region between $r = 0$ and $r = r_0$for which $|\tau_{rz}| < \tau_0$

$$2\pi r_0\, L\, \tau_0 = (P+f)\,\pi\, r_0^2\, L \therefore \tau_0 = \frac{(P+f)\, r_0}{2}, \; or \; r_0 = \frac{2\,\tau_0}{P+f} \tag{2.2.4}$$

Here, $P = -\frac{\partial p}{\partial z}$.

Also by using the condition $\tau_{rz} = \tau_h at r = h$ (Bird et al.[45]), we obtained as:

$$P = \frac{2\,\tau_h}{h}.$$

Hence we obtained as:

$$\frac{r_0}{h} = \frac{\tau_0}{\tau_h} = \tau, \; 0 < \tau < 1. \tag{2.2.5}$$

Using Eq. (2.2.5) along with $r = r_0$in Eq. (2.2.3), we get the plug velocity (see ref.[43–44]) as:

$$u_p = \left[-\frac{1}{6}r_0^2 - \frac{4}{3}r_0^{\frac{1}{2}}\,h^{\frac{3}{2}} + \frac{1}{2}h^2 + h\,r_0\right]\frac{\left(-\frac{\partial p}{\partial z} + f\right)}{2\mu}, \tag{2.2.6}$$

There are several ways to observe the flow flux Q of the fluid:

$$Q = 2\left[\int_0^{r_0} u_p\, r\, dr + \int_{r_0}^{h} u\, r\, dr\right], \tag{2.2.7}$$

$$\therefore Q = \left[-\frac{1}{168}r_0^4 - \frac{2}{7}r_0^{\frac{1}{2}}\,h^{\frac{7}{2}} + \frac{1}{8}h^4 + \frac{1}{6}h^3 r_0\right]\frac{\left(-\frac{\partial p}{\partial z} + f\right)}{\mu}. \tag{2.2.8}$$

The following dimensionless amounts were employed:

$$\begin{Bmatrix} r' = \dfrac{r}{R_0},\; r'_0 = \dfrac{r_0}{R_0}, \delta' = \dfrac{\delta}{R_0}, H = \dfrac{h}{R_0}, z' = \dfrac{z}{L}, \tau'_0 = \dfrac{\tau_0}{\mu\left(\dfrac{c}{R_0}\right)}, d' = \dfrac{d}{R_0}, \\ u' = \dfrac{u}{c}, \tau'_{rz} = \dfrac{\tau_{rz}}{\mu\left(\dfrac{c}{R_0}\right)}, L'_0 = \dfrac{L_0}{R_0}, Q' = \dfrac{Q}{cR_0^2}, p' = \dfrac{p}{\dfrac{\mu c\, L_0}{R_0^2}}, R' = \dfrac{R}{R_0}. \end{Bmatrix}. \tag{2.2.9}$$

Eq. (2.2.8) results from Eq. (2.2.9) as:

$$Q = \left[-\frac{1}{168}r_0^4 - \frac{2}{7}r_0^{\frac{1}{2}}\,H^{\frac{7}{2}} + \frac{1}{8}H^4 + \frac{1}{6}H^3 r_0\right]\left(-\frac{\partial p}{\partial z} + f\right). \tag{2.2.10}$$

Eq. (2.2.10) can be written as follows:

$$\frac{\partial p}{\partial z} = f - \frac{Q}{\left[-\frac{1}{168}r_0^4 - \frac{2}{7}r_0^{\frac{1}{2}}\,H^{\frac{7}{2}} + \frac{1}{8}H^4 + \frac{1}{6}H^3 r_0\right]}. \tag{2.2.11}$$

Eq. (2.2.11) computes the pressure difference Δp lengthways of the whole distance of the pipe as:

$$\Delta p = \int_0^1 \frac{\partial p}{\partial z}dz = \int_0^1 \left\{f - \frac{Q}{\left[-\frac{1}{168}r_0^4 - \frac{2}{7}r_0^{\frac{1}{2}}\,H^{\frac{7}{2}} + \frac{1}{8}H^4 + \frac{1}{6}H^3 r_0\right]}\right\}dz. \tag{2.2.12}$$

Flow opposition is described as:

$$\lambda = \frac{\Delta p}{Q}. \tag{2.2.13}$$

Starting Eqs. (2.2.12) and (2.2.13), we may infer that

$$\frac{1}{Q}\int_0^1 \left\{f - \frac{Q}{\left[-\frac{1}{168}r_0^4 - \frac{2}{7}r_0^{\frac{1}{2}}\,H^{\frac{7}{2}} + \frac{1}{8}H^4 + \frac{1}{6}H^3 r_0\right]}\right\}dz = \lambda. \tag{2.2.14}$$

Due to the nonappearance of stricture($H = 1$), the pressure reduction is deliberate as:

$$\int_0^1 \left\{f - \frac{Q}{\left[-\frac{1}{168}r_0^4 - \frac{2}{7}r_0^{\frac{1}{2}} + \frac{1}{8} + \frac{1}{6}r_0\right]}\right\}dz = (\Delta p)_n. \tag{2.2.15}$$

Flow impedance is defined as follows when there is no stenosis:

$$\lambda_n = \frac{(\Delta p)_n}{Q}. \tag{2.2.16}$$

The expression is given by Eqs. (2.2.15) and (2.2.16) is as follows:

$$\lambda_n = \frac{1}{Q}\int_0^1 \left\{ f - \frac{Q}{\left[-\frac{1}{168}r_0^4 - \frac{2}{7}r_0^{\frac{1}{2}} + \frac{1}{8} + \frac{1}{6}r_0\right]}\right\} dz. \tag{2.2.17}$$

The normalized opposition of a stream is written as:

$$\frac{\lambda}{\lambda_n} = \overline{\lambda}. \tag{2.2.18}$$

Shear stress is applied to the channel's surface as a consequence of

$$\tau_w = -\mu \frac{\partial u}{\partial r}\bigg|_{r=h}. \tag{2.2.19}$$

Using Eq. (2.2.9) to Eq. (2.2.19), it turns into:

$$\tau_w^{'} = \frac{\tau_w}{\left[\frac{\mu c}{R_0}\right]}. \tag{2.2.20}$$

On the other hand, Eq. (2.2.20), is reduced to

$$\tau_w^{'} = -\frac{\partial u'}{\partial r'}. \tag{2.2.21}$$

Using the dimensionless method, modify Eqs (2.2.5) and (2.2.9) in Eq (2.2.21), and the outcome is

$$f - \frac{Q}{2}\left\{\frac{2r_0^{\frac{1}{2}}H^{\frac{1}{2}} - H - r_0}{\frac{1}{168}r_0^4 + \frac{2}{7}r_0^{\frac{1}{2}} H^{\frac{7}{2}} - \frac{1}{8}H^4 - \frac{1}{6}H^3 r_0}\right\} = \tau_w. \tag{2.2.22}$$

Eq. (2.2.22) is used to determine the shear stress at the surface in the nonappearance of stenosis ($H = 1$) as follows:

$$f - \frac{Q}{2}\left\{\frac{2r_0^{\frac{1}{2}} - 1 - r_0}{\frac{1}{168}r_0^4 + \frac{2}{7}r_0^{\frac{1}{2}} - \frac{1}{8} - \frac{1}{6}H^3 r_0}\right\} = (\tau_w)_n. \tag{2.2.23}$$

It is possible to calculate the normalized surface shear stress as follows:

$$\frac{\tau_w}{(\tau_w)_n} = \overline{\tau}_w. \tag{2.2.24}$$

3. Computational results

When analyzing blood flow via a stenosed artery, two critical factors are resistance to flow and wall shear stress. Investigative results for liquid velocity(u), flow opposition $()\overline{\lambda})$, and wall shear stress ($\overline{\tau}_w$) are shown in Eqs. (2.2.3), (2.2.18), and (2.2.24), respectively. The several restrictions on stream opposition, wall shear stress, and fluid velocity are numerically estimated with the help of MATHEMATICA, and the results are then visualized using graphs.

3.1. Opposition to the flow

Opposition to stream is demonstrated to yield greater values for lifeblood vessels with larger stenosis heights, nevertheless, the reverse is true for arteries with lesser stenosis elevations. It's essential to understand the physical foundation for these findings. The stenosis area's stopped liquid quickly moves toward the core flowing area. As a result, the liquid encounters a brief obstruction in the pre-stenotic region before decreasing in size in the post-stenotic region. The effects of impedance on various limitations, including stenosis height (δ), are depicted in Figs. 2–5. When there is stenosis, it is observed that the radial distance (r) of the linked region increases, and the flow impedance (δ) increases (see Fig. 2,3). The impedance rises when the Casson liquid possesses non-Newtonian characteristics.

According to Fig. 4 and 5, as the angle of bent (θ) increases, the flow

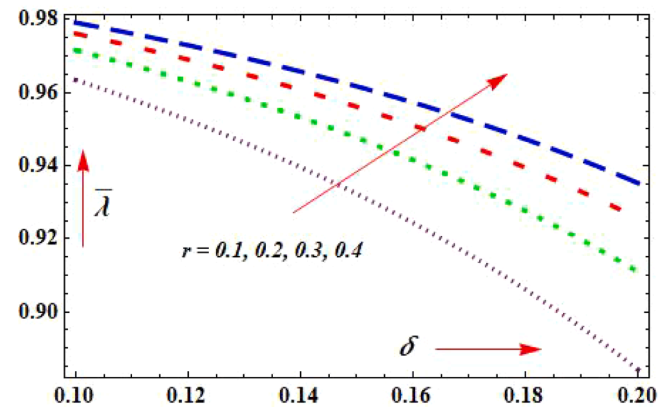

Fig. 2. Design of $\overline{\lambda}$ for r through $\theta = \pi/6$, $Q = 0.1$, $d = 0.2$, $L_0 = 0.4$, $F = 0.1$.

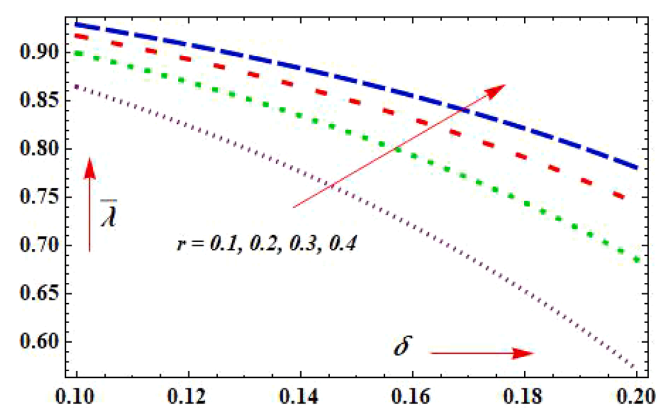

Fig. 3. Design of $\overline{\lambda}$ for r through $\theta = \pi/6$, $Q = 0.1$, $d = 0.2$, $L_0 = 0.4$, $F = 0.3$.

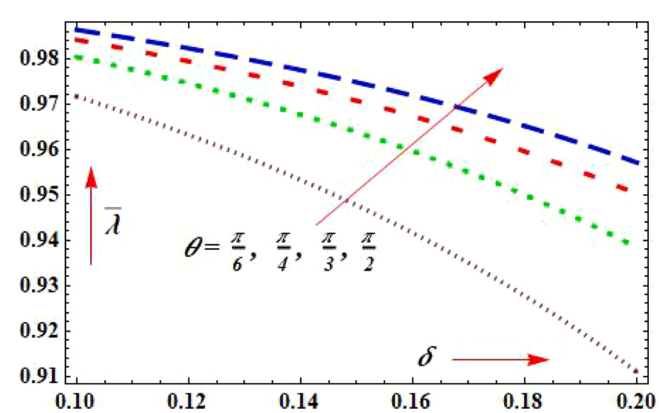

Fig. 4. Design of $\overline{\lambda}$ for θthrough $r = 0.2$, $Q = 0.1$, $d = 0.2$, $L_0 = 0.4$, $F = 0.1$.

impedance ($\overline{\lambda}$) rises for the height of the stenosis (δ). These findings show that the decreased lumen size of the slanted artery, which influences the flow, causes a significant change in the plug flow radius. In comparison to arteries that are not inclined, the plug flow radius is larger in sloped arteries. It supports Srivastava's claims.[33] These results are in line with earlier findings by[5,12,27] and they also support the results of experiments by Bureau et al.[39] and McMillan et al.[40] on fluid flow resistance.

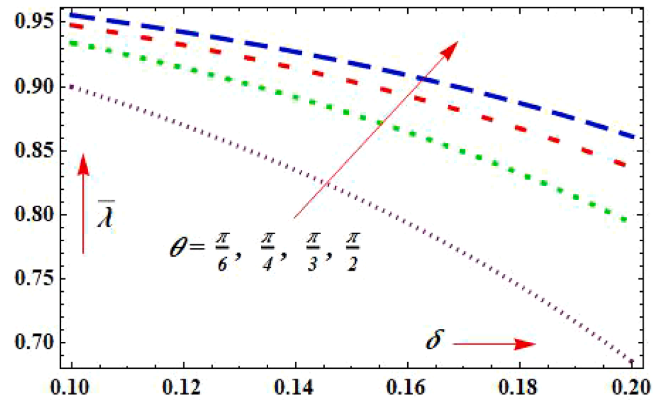

Fig. 5. Design of $\bar{\lambda}$ for θthrough $r = 0.2$, $Q = 0.1$, $d = 0.2$, $L_0 = 0.4$, $F = 0.3$.

3.2. Shear-stress of the wall

The tiny arteries and arterioles must be understood in the context of wall shear stress. The arteries are affected by the pressure gradient and wall shear stress, which over time makes them more rigid and less flexible. The arterial wall ruptures in these injured arteries when they are subjected to high blood pressure. The effects of surface shear stress ($\bar{\tau}_w$) on various restrictions with a height of stenosis are shown in Figs. 6–9. As r of the linked flowing area increases, it is demonstrated that surface shear stresses both decrease and increase in response to the elevation of stenosis (see Fig. 6,7). According to Figs. 8–9, the height of the stenosis (δ) causes an increase in the proclivity angle (θ), which causes an increase in wall shear stress. The numerical findings of Young,[1] Chakraborty and Mandal,[13] and Prasad and Radhakrishnamacharya[30] are in agreement with these findings. In the case of fluid wall shear stress, our results concur with those of Bureau et al.[39] and McMillan[40] experiments.

3.3. Fluid velocity

Figs. 10–13 show how different restrictions impact the fluid's velocity (u). As stenosis height (δ) rises, it is demonstrated that fluid velocity (u) drops (see Figs. 10 and 11). It has been noted that fluid velocity (u) is highest in the tube's middle and declines toward the wall before reaching zero at the tube's wall. It is obvious that the regular artery moves at a higher speed than the stenosed artery. The effects of the proclivity angle are depicted in Figs. 12–15. It has been observed that in stenosis conditions, the fluid's velocity (u) increases an angle of inclination (θ) increase. Additionally, it has been noticed that the fluid velocity is seen to be decreasing as the radial distance and stenosis height

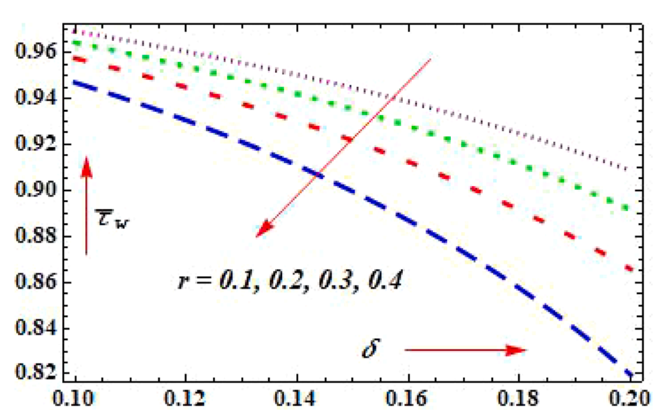

Fig. 6. Design of $\bar{\tau}_w$ for r through $Q = 0.1$, $d = 0.2$, $\theta = \pi/6$, $L_0 = 0.4$, $F = 0.1$.

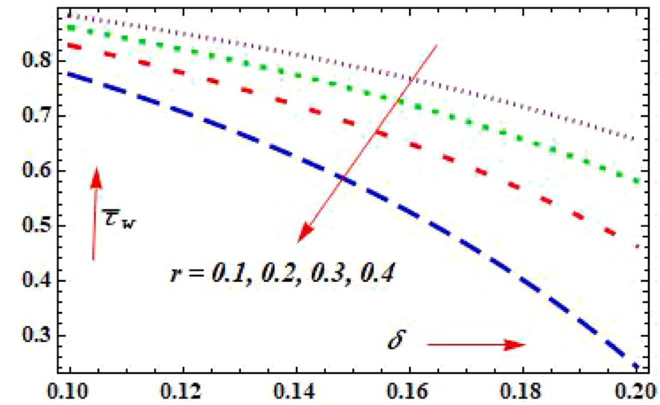

Fig. 7. Design of $\bar{\tau}_w$ for r through $Q = 0.1$, $d = 0.2$, $\theta = \pi/6$, $L_0 = 0.4$, $F = 0.3$.

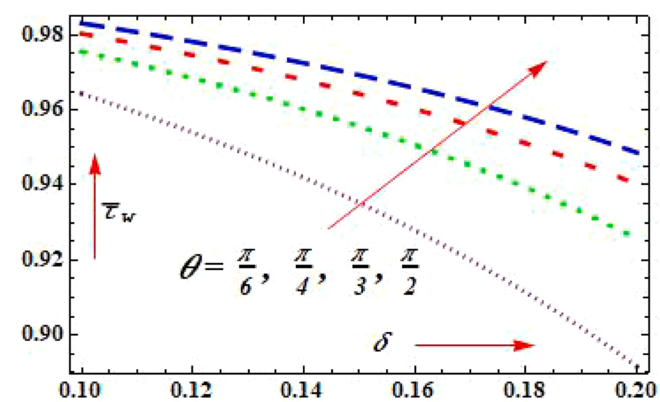

Fig. 8. Design of $\bar{\tau}_w$ for θthrough $Q = 0.1$, $d = 0.2$, $r = 0.2$, $L_0 = 0.4$, $F = 0.1$.

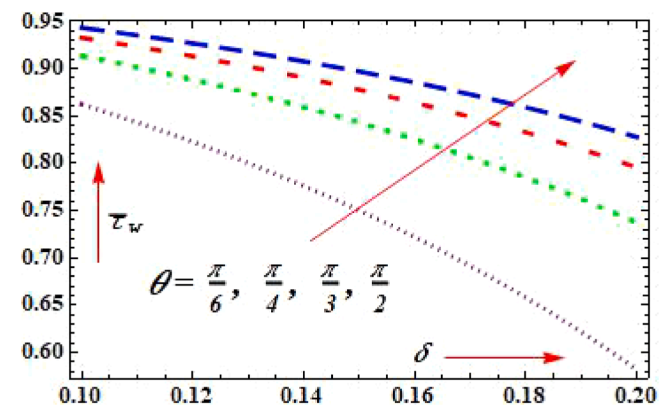

Fig. 9. Design of $\bar{\tau}_w$ for θ through $Q = 0.1$, $d = 0.2$, $r = 0.2$, $L_0 = 0.4$, $F = 0.3$.

increase. These results concur with those made before Young[1] and Chakraborty and Mandal.[13]

4. Concluding observations

The mathematical model of Casson liquid in a steady, consistent tube with overlapping stenosis is examined. The results are represented graphically for varied radial distance, inclination angle, stenosis altitude, and expansion following stenosis values. The main conclusions are as follows:

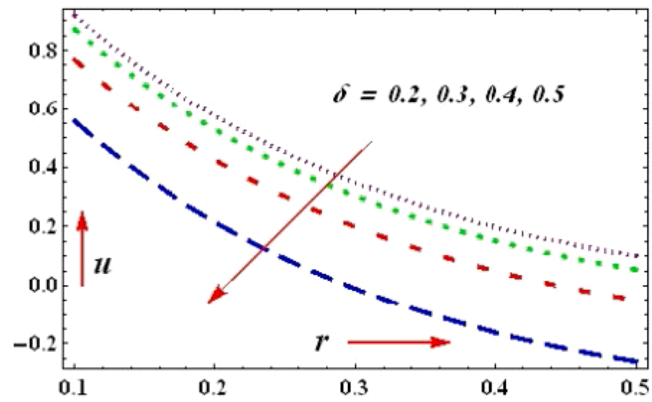

Fig. 10. Design u & r for δ through $z = 0.5$, $d = 0.2$, $\theta = \pi/6$, $L_0 = 0.4$, $F = 0.1$.

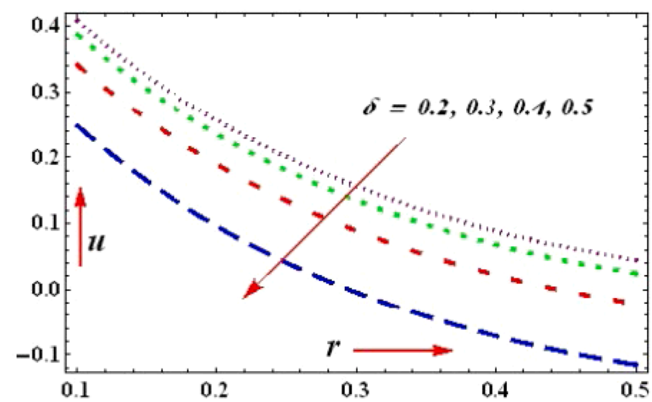

Fig. 11. Design u & r for δ through $z = 0.5$, $d = 0.2$, $\theta = \pi/6$, $L_0 = 0.4$, $F = 0.3$.

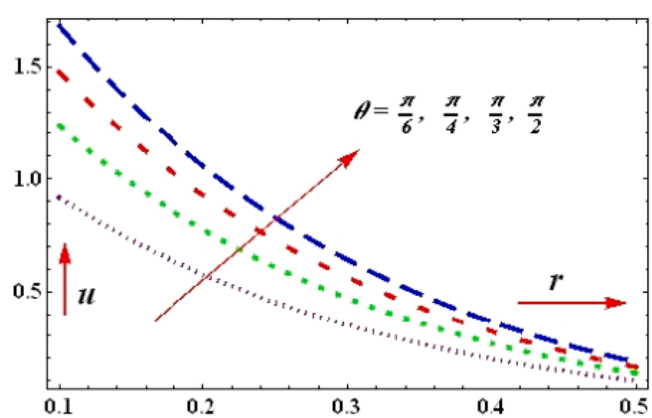

Fig. 12. Design of u & r for θthrough $\delta = 0.3$, $z = 0.5$, $d = 0.2$, $L_0 = 0.4$, $F = 0.1$.

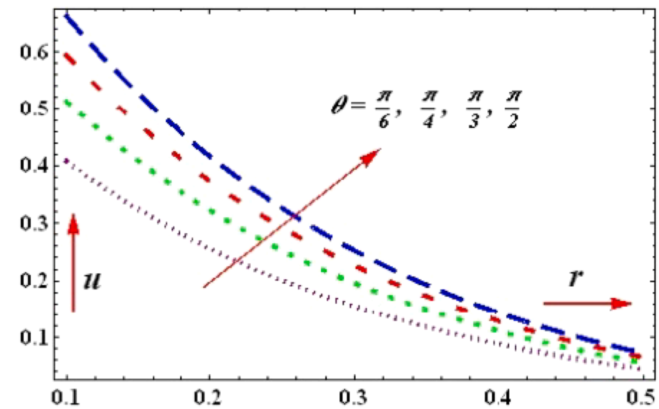

Fig. 13. Design of u & r for θthrough $\delta = 0.3$, $z = 0.5$, $d = 0.2$, $L_0 = 0.4$, $F = 0.3$.

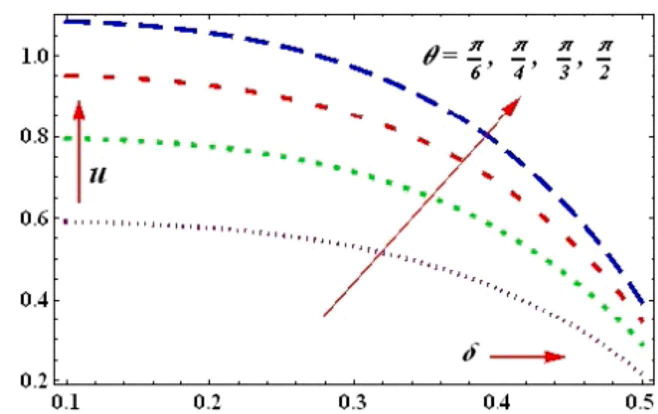

Fig. 14. Design of u & δ for θthrough $r = 0.2$, $z = 0.5$, $d = 0.2$, $L_0 = 0.4$, $F = 0.1$.

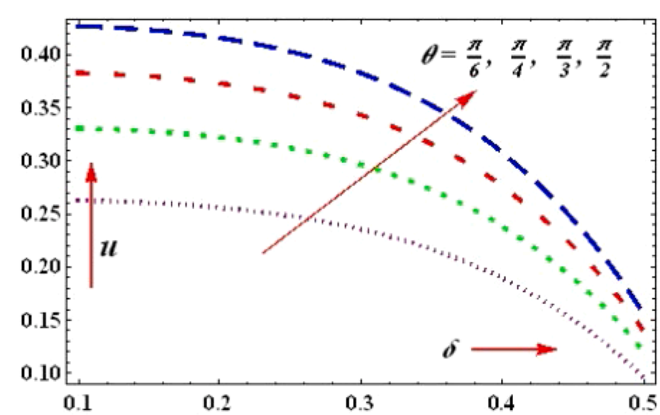

Fig. 15. Design of u & δ for θthrough $r = 0.2$, $z = 0.5$, $d = 0.2$, $L_0 = 0.4$, $F = 0.3$.

- Surface shear stress falls and flowing resistivity rises as the radial length (r) of the linked flowing region increases.
- Concerning the height of stenosis, the surface shear stress and the resistivity to flow increase together with an increase in the proclivity angle.
- As the level of stenosis altitude increases, the blood's velocity decreases.
- The fluid's velocity increases in response to an increase in proclivity angle.
- For heights of stenosis, an increase in the radial length of the linked area results in a decrease in the fluid's velocity.

The above-mentioned discoveries might be applied to improve blood vessel function. Drugs could be administered to people with aberrant blood vessel narrowing using this method. Additionally, the associated discovery of the current physical model will act as a prototype for pharmaceutical and biological researchers engaged in research and development work. This mathematically based work may serve as a biomedical engineering prototype for the use of angioplasty to treat vascular-related disorders.

Declaration of competing interest

The authors declare that they have no known competing financial interests or personal relationships that could have appeared to influence the work reported in this manuscript.

Acknowledgements

This work was supported by BLDE University grant number BLDEU/R&D/RGC/2022-23/3329/1. The authors express gratitude for the financial support extended by the BLDE University, India. They also wish to express their gratitude to the very competent anonymous referees for their valuable comments and suggestions.

References

1. Young DF. Effect of a time dependent stenosis of flow through a tube. *J. Eng. Indust. Trans. ASME*. 1968;90:248–254.
2. Azuma T, Fukushima T. Flow patterns in stenotic blood vessel models. *Biorheol.* 1976;13:337–355.
3. Macdonald DA. On Steady flow through modelled vascular stenosis. *J. Biomech.* 1979;12:13–30.
4. Forrester JH, Young DF. Flow through a conversing diverging tube and its implications in occlusive vascular disease. *J. Biomech.* 1970;3:297–316.
5. Shukla JB, Parihar RS, Rao BRP. Effects of stenosis on non-Newtonian flow through an artery with mild stenosis. *Bull. Math. Biol.* 1980;42:283–294.
6. Perkkio J, Keskinen R. On the effect of the concentration profile of red cells on blood flow in the artery with stenosis. *Bull. Math. Biol.* 1983;45(2):259–267.
7. Misra JC JC, Kar BK. Momentum integral method for studying flow characteristics of blood through a stenosed vessel. *Biorheol.* 1989;26:23–35.
8. Tandon PN, Rana UV, Kawahara M, Katiyar VK. A model for blood flow through stenotic tube. *Int. J. Biomed. Comput.* 1993;32:62–78.
9. Srinivasacharya DS, Srikanth D. Effect of Couple Stresses on the flow in a constricted annulus. *Arch. Appl. Mech.* 2008;78:251–257.
10. Nakamura M, Sawada T. Numerical study on the flow of a non-Newtonian fluid through an axisymmetric stenosis. *J. Biomech. Eng.* 1988;110:137–143.
11. Sharma MK, Sharma PR, Nasha V. Pulsatile MHD arterial blood flow in the presence of double stenosis. *J. Appl. Fluid Mech.* 2013;6(3):331–338.
12. Verma N, Parihar RS. Effect of magneto-hydrodynamics and haematocrit on blood flow in an artery with multiple mild stenosis. *Int. J. Appl. Math. Comput.* 2009;1(1): 30–46.
13. Chakravarty S, Mandal TK. Mathematical modelling of blood flow through an overlapping stenosis. *Math. Comput. Model.* 1994;19:59–73.
14. Chakravarty S, Mandal TK. A nonlinear two-dimensional model of blood flow in an overlapping arterial stenosis subjected to body acceleration. *Math. Comput. Model.* 1996;24(1):43–58. https://doi.org/10.1016/0895-7177(96)00079-9.
15. Srivastava VP, Mishra S, Rastogi R. Non-Newtonian arterial blood flow through an overlapping Stenosis. *Appl. Appl. Math. Int. J.* 2010;5(1):225–238.
16. Srivastava VP, Vishnoi R, Mishra S, Sinha P. A Two-layered non-Newtonian arterial blood flow through an overlapping constriction. *Appl. Appl. Math. Int. J.* 2011;6(11): 1781–1797.
17. Riahi DN, Roy R, Cavazos S. On arterial blood flow in the presence of an overlapping stenosis. *Math. Comput. Model.* 2011;54:2999–3006. https://doi.org/10.1016/j.mcm.2011.07.028.
18. Haghighi AR, Shahbazi MA. Mathematical modeling of micropolar fluid flow through an overlapping arterial stenosis. *Int. J. Biomath.* 2015;8(4), 1550056. https://doi.org/10.1142/S1793524515500564.
19. Reddy JVR, Srikanth D. The polar fluid model for blood flow through a tapered artery with overlapping stenosis: effects of catheter and velocity Slip. *Appl. Bionics Biomech.* 2015;174387. https://doi.org/10.1155/2015/174387.
20. Zaman A, Ali N, Beg OA. Unsteady magnetohydrodynamic blood flow in a porous-saturated overlapping stenotic artery: num. model. *J. Mech. Medicine Biol.* 2016;16 (4), 1650049. https://doi.org/10.1142/S0219519416500494.
21. Sharma MK, Nasha V, Sharma PR. A study for analyzing the effect of overlapping stenosis and dilatation on non-Newtonian blood flow in an inclined artery. *J. Biomed. Sci. Eng.* 2016;9:576–596. https://doi.org/10.4236/jbise.2016.912050.
22. Zain NM, Ismail Z. Modelling of Newtonian blood flow through a bifurcated artery with the presence of an overlapping stenosis. *Mal. J. Fund. Appl. Sci.* 2017;1: 304–309. https://doi.org/10.11113/mjfas.v13n4-1.866.
23. Nadeem S S, IJAZ S. Nanoparticles analysis on the blood flow through a tapered catheterized elastic artery with overlapping stenosis. *Eur. Phys. J. Plus.* 2014;129: 249. https://doi.org/10.1140/epjp/i2014-14249-1.
24. Mekheimer KS, EL Elnaqeeb EL, Kot TMA, Alghamdi F. Simultaneous effect of magnetic field and metallic nanoparticles on a micropolar fluid through an overlapping stenotic artery: blood flow model. *Phys. Essays*. 2016;29(2):272–283. https://doi.org/10.4006/0836-1398-29.2.272.
25. Scottblair GW. An equation for the flow of blood, plasm and serum through glass capillaries. *Nature.* 1959;183(4):613–625.
26. Bali R, Awasthi U. A Casson Fluid Model for Multiple Stenosed Artery in the presence of magnetic field. *Appl. Math.* 2012;3:436–441.
27. Chaturani P, Ponnalagusamy R. Pulsatile flow of Casson fluid through stenosed arteries with applications to blood flow. *Biorheol.* 1986;23:499–511.
28. Mustafa M, Hayat T, Pop I, Aziz A. Unsteady boundary layer flow of a Casson fluid due to an impulsively started moving flat plate. *Heat Transf. Asian Res.* 2011;40(6): 563–576.
29. Vajravelu K, Sreenadh S, Devaki P, Prasad KV. Peristaltic pumping of a Casson fluid in an elastic tube. *J. Appl. Fluid Mech.* 2016;9(4):1897–1905.
30. Prasad MK, Radhakrishnamacharya G. Flow of Herschel-Bulkley fluid through an inclined tube of non-uniform cross-section with multiple stenosis. *Arch. Mech.* 2008; 60:161–172.
31. Gudekote M, Choudhari R. Slip effect on peristaltic transport of Casson fluid in an inclined elastic tube with porous walls. *J. Adv. Res. Fluid Mech. Therm. Sci.* 2018;43 (1):67–80.
32. Umadevi C, Dhange M, Haritha B, Sudha T. Flow of blood mixed with copper nanoparticles in an inclined overlapping stenosed artery with magnetic field. *Case Stud. Therm. Eng.* 2021;25, 100947.
33. Srivastava N. The Casson fluid model for blood flow through an inclined tapered artery of an accelerated body in the presence of magnetic field. *Int. J. Biomed. Eng. Technol.* 2014;15(2):198–210.
34. Gupta AK, Gupta GD. Unsteady blood flow in an artery through a non-symmetrical stenosis. *Acta Cienc. Indica.* 2001;XXVII M(2):137–142.
35. Pralhad RN, Schultz DH. Modelling of arterial stenosis and its applications to Blood diseases. *Math. Biosci.* 2004;190:203–220.
36. Kumar H, Chandel RS, Sanjeev K, Sanjeet K. A mathematical model for different shapes of stenosis and slip velocity at the wall through mild stenosis artery. *Adv. Appl. Math. Biosci.* 2014;5(1):9–18.
37. Sankad G, Dhange M. Effect of chemical reactions on dispersion of a solute in peristaltic motion of Newtonian fluid with wall properties. *Malaysian J. Math. Sci.* 2017;11(3):347–363.
38. Otto CM. Aortic stenosis: even mild disease is significant. *Eur. Heart J.* 2004;25(3): 185–187. https://doi.org/10.1016/j.ehj.2003.12.010.
39. Mureau M, Healy JC, Bourgoin D, et al. Rheological hysteresis of blood at low shear rate. *Biorheol.* 1979;16:7–100.
40. Mcmillan DE, Strigberger J, Utterback NG. Rapidly recovered transient flow resistance: a newly discovered properties of blood. *Am. J. Physiol.* 1987;253(4): H919–H926. https://doi.org/10.1152/ajpheart.1987.253.4.H919.
41. Pratumwal Y, Limtrakaran W, Muengtaweepongsa S, Phakdeesan P, Intharakham K. Whole blood viscosity modelling using power las, Casson, and Carreau Yasuda models interegrated with image scanning U-tube viscometer technique. *Songklanakarin J. Sci. Technol.* 2017;39(5):625–631.
42. Vajravelu K, Sreenadh S, Ramesh BV. Peristaltic transport of a Herschel-Bulkley fluid in an inclined tube. *Int. J. Nonlin. Mech.* 2005;40:83–90.
43. Chaturani P, Ponalagusamy R. Pulsatile flow of Casson fluid through stenosed arteries with application to blood flow. *Biorheol.* 1986;23:499–511.
44. Siddiqui AM, Farooq AA, Rana MA. A mathematical model for the flow of a Casson fluid due to metachronal beating of Cilia in a tube. *Sci. World J.* 2015;487816:1–12.
45. Bird RB, Stewart WE, Lightfoot EN. *Transport Phenomena*. New York: Wiley; 1976.
46. Abdul-Wahab MS, Abdul Sattar J, Saif AA. Studying the effects of electro-osmotic and several parameters on blood flow in stenotic arteries using CAGHPM. *Partial Differ. Equ. Appl. Math.* 2024;11, 100767.
47. Imitaz A, Aamina A, Ali F, Khan I, Nisar KS. Two-phase flow of blood with magnetic dusty particles in cylindrical region: a Caputo Fabrizio fractional model. *Comput. Mater. Con.* 2021;66(3):2253–2264.
48. Sankad G, Ishwar M, Dhange M. Varying temperature and thermal radiation effects on MHD boundary layer liquid flow containing gyrotactic microorganisms. *Partial Differ Equ Appl Math.* 2021;4, 100092.
49. Ali F, Haq F, Khan N, Imtiaz A, Khan I. A time fractional model of hemodynamic two-phase flow with heat conduction between blood and particles: applications in health science. *Waves Random Complex Media*. 2023:2–28.
50. Roshid MM, Bairagi T, Roshid HO, Rahman MM. Lump, interaction of lump and kink and solitonic solution of nonlinear evolution equation which describe incompressible viscoelastic Kelvin–Voigt fluid. *Partial Differ Equ Appl Math*. 2022;5, 100534.
51. Imtiaz A, Foong OM, Aamina A, Khan N, Ali F, Khan I. Generalized model of blood flow in a vertical tube with suspension of gold nanomaterials: applications in the cancer therapy. *Comput Mater Con*. 2020;65(1):171–192.